A Trajectory Approach to Analyzing the Ingredients Associated with Heavy Winter Storms in Central North Carolina

CHRISTOPHER M. FUHRMANN AND CHARLES E. KONRAD II

Southeast Regional Climate Center, Department of Geography, University of North Carolina at Chapel Hill, Chapel Hill, North Carolina

(Manuscript received 10 August 2012, in final form 23 January 2013)

ABSTRACT

Winter storms, namely snowstorms and ice storms, are a major hazard and forecasting challenge across central North Carolina. This study employed a trajectory approach to analyze the ingredients (i.e., temperature, moisture, and lift) associated with heavy snowstorms and ice storms that occurred within the Raleigh, North Carolina, National Weather Service forecast region from 2000 to 2010. The Hybrid Single-Particle Lagrangian Integrated Trajectory (HYSPLIT) tool was used to calculate 72-h backward (i.e., upstream) air parcel trajectories from three critical vertical pressure levels at the time and location of heaviest precipitation for each storm. Analysis of composite trajectories revealed the source regions and meteorological properties of air parcels associated with heavy winter storms. Adiabatic and diabatic contributions to air parcel temperature and moisture content were also estimated along each trajectory to assess the physical processes connected with heavy winter precipitation in the region. Results indicate that diabatic warming and cooling contribute significantly to the vertical temperature profile during heavy winter storms and therefore dictate the resulting precipitation type. The main source of diabatic warming is fluxes of sensible and latent heat within the marine atmospheric boundary layer over the Gulf Stream. These fluxes contribute to a warming and moistening of air parcels associated with heavy ice storms. In contrast, heavy snowstorms are characterized by diabatic cooling in the lower troposphere above the marine atmospheric boundary layer. The most significant moisture source for heavy snowfall is the Caribbean Sea, while heavy ice storms entrain moisture from the Gulf of Mexico and Gulf Stream region near the Carolina coast.

1. Introduction

Precipitation has long been considered one of the greatest forecasting challenges (Fritsch et al. 1998). During the winter, precipitation type (i.e., rain, snow, and freezing rain) is especially difficult to forecast because it depends on the details of the vertical temperature profile in the lower troposphere. In the southeast United States, precipitation-type forecasting is further complicated by the unique geography of the region, which plays an important role in the evolution of the vertical temperature profile through complex interactions involving the synoptic-scale circulation, the regional topography (i.e., Appalachian Mountains), and nearby bodies of water (i.e., the Gulf of Mexico and Atlantic Ocean) (Keeter et al. 1995; Fig. 1). Cold and warm air masses often intersect across parts of the Southeast, further complicating the vertical temperature profile. Indeed, many winter precipitation events in the region are often near a ''tipping point'' with regard to temperature (i.e., near 0°C); therefore, subtle changes in the vertical temperature profile can lead to significant changes in precipitation type and intensity. Moreover, some of the physical processes that affect the vertical temperature profile are not fully represented in numerical weather prediction models, which can result in major forecast ''busts'' (Lackmann et al. 2002). These forecast busts are important, as they can exacerbate already significant societal impacts. These include economic losses, property damage, disruption to utilities and transportation, power outages, school and business closings, injury, and loss of life (Fuhrmann et al. 2009).

Over the past several decades, a number of conceptual models and forecast methods for winter precipitation in central North Carolina have been developed through a collaborative enterprise between the Raleigh, North

Corresponding author address: Dr. Christopher M. Fuhrmann, Southeast Regional Climate Center, Dept. of Geography, University of North Carolina at Chapel Hill, Chapel Hill, NC 27599-3220.
E-mail: fuhrmann@unc.edu

DOI: 10.1175/WAF-D-12-00079.1

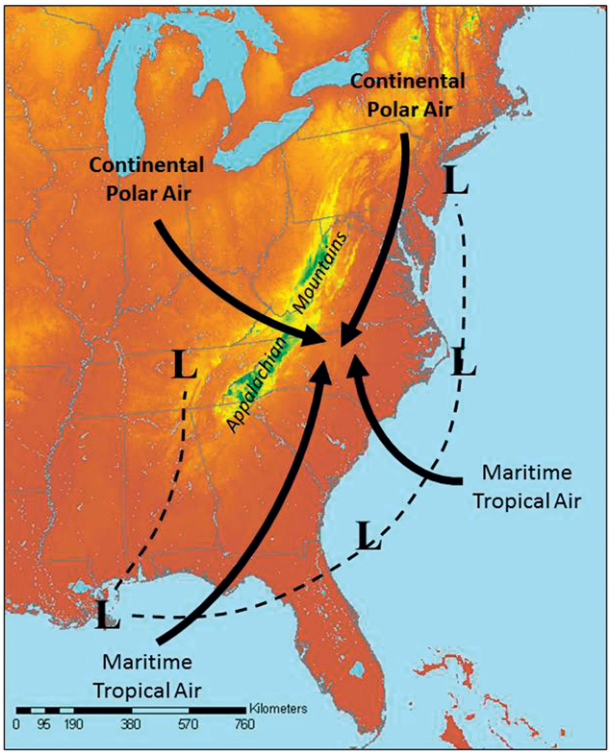

FIG. 1. Schematic map illustrating the regional topography and the main cyclone tracks (L) and air masses connected with winter precipitation in central NC. [Reproduced from Keeter et al. (1995).]

Carolina, National Weather Service (hereafter Raleigh NWS) and atmospheric scientists at North Carolina State University (Waldstreicher 2005). The most recent project involving winter precipitation, which ended in 2006, focused on improving quantitative precipitation forecasts (QPFs). Conceptual models were developed to illustrate relationships between QPF and various atmospheric features and processes, including coastal cyclogenesis, upstream convection, cold-air damming, and lower-tropospheric potential vorticity maxima (Lackmann 2006). In the present study, we build upon these methods and models by using a trajectory approach to identify the upstream atmospheric features and physical processes that contribute both to precipitation type and intensity across central North Carolina. A trajectory can be defined as simply the path that an air parcel takes over space and time. With improvements in model resolution and parameterization schemes, calculating air parcel trajectories is considered a more accurate method than previously used storm-relative isentropic analyses to envision the airflow associated with midlatitude weather systems (Schultz 2001). Moreover, trajectory analysis represents an underutilized method and framework for analyzing the physical processes that result in heavy winter precipitation. One exception is Moore et al. (2005), who used high-resolution model data to produce mesoscale trajectories of airstreams connected with two heavy banded snowfall events in the upper Midwest. They concluded that the ''belts'' of air portrayed in the trajectory models aided in the visualization of the features and processes associated with heavy banded snowfall, which is a major forecasting challenge in the region. Therefore, in an operational setting, trajectory analysis may be useful in determining the source regions of various meteorological parameters (e.g., temperature, moisture), tracing the evolution of their properties back across space and time, and relating changes in their properties to the physical processes that contribute to precipitation through identification of upstream surface and atmospheric features along each trajectory segment (Stohl 1998).

The Hybrid Single-Particle Lagrangian Integrated Trajectory (HYSPLIT) tool, developed and maintained by the National Oceanic and Atmospheric Administration's (NOAA) Air Resource Laboratory (ARL), is used in this study to calculate back trajectories associated with a sample of heavy snowstorms and ice storms that occurred within the Raleigh NWS forecast region from 2000 to 2010. This work is guided by the following research questions: 1) What are the space–time characteristics of air parcels that are advected into the atmospheric column of an evolving winter storm? 2) How do these characteristics affect the meteorological properties of the air parcels as they approach the region of heavy winter precipitation? 3) What are the physical processes (e.g., diabatic warming) and upstream features (e.g., Gulf Stream current) that operate on the air parcels as they approach the region of winter precipitation? 4) How do the identified characteristics of the air parcels relate to the type and intensity of precipitation observed?

The paper is organized as follows. Section 2 describes the data and methods used, beginning with a discussion of the study area, followed by the procedures used to select and classify winter storms, compute back trajectories and meteorological variables along each trajectory segment, and compute comparative trajectories for a sample of storms. Analyses of trajectories are presented separately for heavy snowstorms (section 3) and heavy ice storms (section 4). A summary of the major findings and applications to operational forecasting, as well as a discussion of limitations and avenues for future work, are presented in section 5.

2. Data and methods

This study focuses on the Raleigh NWS County Warning Area (CWA), a contiguous region covering 31

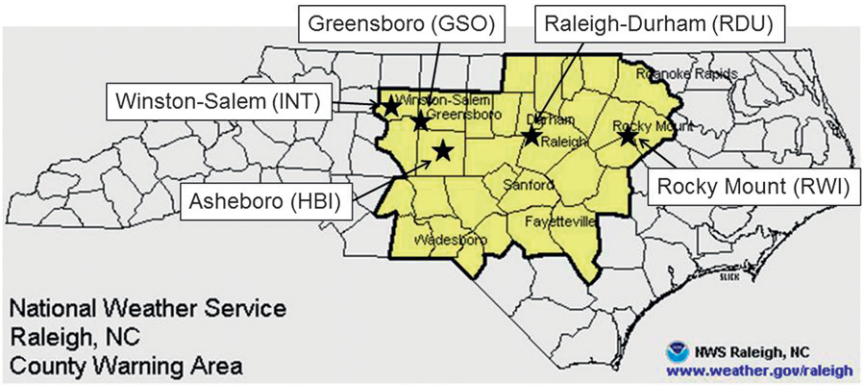

FIG. 2. County-level map of NC with the Raleigh NWS CWA highlighted in yellow. Stars indicate the first-order stations and ending locations (with labels) for the trajectory analyses.

counties in central North Carolina (Fig. 2). The Raleigh CWA is a highly populated area with several major urban and transportation corridors. As a result, the societal impacts from winter storms in the region can be significant (Fuhrmann et al. 2009). Moreover, the climatological position of the precipitation-type transition zone (e.g., rain–snow line) extends across the CWA (Keeter et al. 1993). Therefore, most forecasts of precipitation type in the region are predicated on the accurate prediction of the transition zone, which is tied to the vertical thermal profile (Keeter et al. 1995).

The Raleigh NWS maintains an online archive of detailed precipitation maps of winter storms affecting the CWA (http://www.erh.noaa.gov/rah/events). These maps are produced using daily snowfall data from the Cooperative Observer (COOP) network as well as hourly precipitation data from first-order airport stations. This level of detail allows for the identification of locations with the heaviest precipitation and for demarcating regions of different precipitation types. Using this archive, the heaviest events from 2000 to 2010 were selected for analysis. This period was chosen for a few reasons. First, the level of detail of the precipitation maps produced by the Raleigh NWS has improved over the last decade due to the inclusion of more station observations. Second, the spatial resolution of the meteorological dataset used in the trajectory analyses is maximized during this period (discussed later in this section). Finally, a total of 60 winter storms were documented by the Raleigh NWS over this period, providing a reasonably large sample from which the heaviest events could be selected for analysis. Only the heaviest events were examined because they were generally associated with the greatest societal impacts (Fuhrmann et al. 2009). Since the study area corresponds to the Raleigh CWA, the heaviest events were defined based on NWS criteria used to forecast and warn for heavy snow and ice (hereafter referred to as snowstorms and ice storms). In the southeast United States, most NWS offices, including Raleigh, define a heavy snowstorm as one that produces at least 4 in. (10.2 cm) of snow in at least one county within the CWA (B. Locklear 2009, personal communication). In the case of an ice storm, the NWS will issue an ice storm warning if at least 0.25 in. (0.6 cm) of ice is expected to accumulate in at least one county within the CWA. In cases where ice accumulation resulted from both freezing rain and sleet, the Raleigh NWS typically reported the combined total from both types on their precipitation maps. In these cases, the threshold for an ice storm, as defined in this study, was changed to 0.5 in. (1.3 cm). Precipitation maps of the original 60 storms from 2000 to 2010 were examined to determine if at least one observation was made in the Raleigh NWS CWA that met the above criteria for either a snowstorm or an ice storm. This yielded a total of eight snowstorms and seven ice storms (Table 1). Hourly data from the nearest first-order station were also examined to confirm the maximum storm-total precipitation and determine the duration for each storm. Several factors and processes can influence snowfall measurements, including sublimation, compaction, melting, blowing and drifting, and snow density (Kocin and Uccellini 2004). Measurements of ice accumulation at first-order stations are also sensitive to variations in precipitation rate, droplet size, wind speed, and wind direction (Ryerson and Ramsay 2007). A more detailed discussion of the limitations associated with snowfall and ice accumulation measurements can be found in Fuhrmann (2011).

In this study, back trajectories were calculated using version 4.9 of the HYSPLIT tool (Draxler and Rolph 2011). Stohl (1998) discussed some of the limitations of trajectory analyses. In general, the path of an air parcel along a trajectory is sensitive to the initial conditions of

TABLE 1. List of snowstorms and ice storms examined in this study. Values in boldface are for combined sleet and freezing rain totals. Locations for the trajectory analyses are shown in Fig. 1.

Event	Location for trajectory analysis	Maximum event-total precipitation (in.)	Duration (h)
Snowstorms			
24–25 Jan 2000	RDU	20	22
3–4 Dec 2000	RWI	10	12
3–4 Jan 2002	RDU	14	27
26–27 Feb 2004	HBI	20	18
26 Dec 2004	RWI	10	13
20 Jan 2009	RDU	8	13
1–2 Mar 2009	GSO	7	10
26–27 Dec 2010	RWI	14	20
Ice storms			
30 Jan 2000	GSO	**0.75**	24
4–5 Dec 2002	RDU	1.50	18
16–17 Feb 2003	INT	**3.00**	30
26–27 Feb 2003	GSO	1.00	32
14 Dec 2003	GSO	**1.00**	20
25–26 Jan 2004	GSO	**6.00**	24
29–30 Jan 2005	GSO	0.25	16

the model data, uncertainties in the wind field used to calculate air parcel motions, and interpolation related to model resolution. Air parcel position errors of up to 20% have been noted for trajectories lasting longer than 24 h (Stohl 1998). One way to test the sensitivity of a trajectory model to the meteorological input data is to produce an ensemble (Draxler 2003). This method involves performing multiple model runs with slightly different initial conditions and then assessing the variance in the output trajectory characteristics. Fuhrmann (2011) performed an ensemble analysis of several of the events examined in the present study and found that the trajectory model was able to resolve key aspects of winter precipitation, such as temperature and moisture, and that ensemble members with varying trajectory paths were distinguished by their meteorological properties.

The meteorological dataset used to initialize each HYSPLIT run was the National Centers for Environmental Prediction's (NCEP) Eta Data Assimilation System (EDAS), which became the North American Mesoscale Model (NAM) Data Assimilation System (NDAS) in 2005 (Rogers et al. 2009). The EDAS/NDAS system is commonly used in trajectory studies and combines meteorological observations with short-term weather forecasts to produce dynamically consistent estimates of the state of the atmosphere. EDAS/NDAS contains several basic fields, including the u and v components of the horizontal wind, temperature, and relative humidity that are archived every 3 h across a North American grid. NOAA/ARL began archiving EDAS/NDAS data in 1997 with a spatial resolution of 80 km. In 2004, the spatial resolution increased to 40 km. Hondula et al. (2009) used EDAS/NDAS to examine a large sample of trajectories in HYSPLIT during a 4-month overlap period in the datasets (January–April 2004) and found no statistically significant differences in the horizontal or vertical extents of the trajectories. Therefore, both versions were used in this study to produce a continuous record from 2000 to 2010. The higher-resolution dataset was used for events that occurred during the overlap period. The use of EDAS/NDAS over other available datasets in the ARL archive was based on two factors. First, EDAS/NDAS provided the highest model resolution over the study period (2000–10). Second, the original EDAS system was an integral part of the operational Eta Model (Black 1994), which had been used routinely to forecast winter precipitation across the southeast United States, including the Raleigh CWA, since the early 1990s until it was replaced by the Weather Research and Forecasting version of the Nonhydrostatic Mesoscale Model (WRF-NMM; Rogers et al. 2009). Therefore, by using the EDAS/NDAS model system, the results of this study should be directly applicable to forecasters in the region.

A backward-trajectory analysis was undertaken for each snowstorm and ice storm in order to assess the influence of the upstream environment on the ingredients (i.e., temperature, moisture, lift) and physical processes that contribute to winter precipitation in central North Carolina. The HYSPLIT tool was used to calculate 72-h back trajectories for air parcels at three critical levels over the location of heaviest precipitation: 1) near-surface trajectories (ending at 975 hPa), 2) warm layer zone trajectories (ending at 850 hPa), and 3) dendritic growth zone trajectories ending at the mean pressure with temperature between −13° and −17°C, where precipitation production is especially high (Fig. 3). The location of heaviest precipitation was determined by examining the NWS precipitation map for each storm. The time of heaviest precipitation was determined by examining the hourly precipitation time series for the first-order station nearest the location of heaviest precipitation. Specifically, the time (hour) of heaviest precipitation was identified as the middle hour of the 3-h period with the heaviest aggregate precipitation in the time series. This procedure was used because more than 50% of the total precipitation observed over most of the events in this study occurred in a 3-h period of time. The 72-h duration was selected to appropriately assess antecedent synoptic and subsynoptic-scale circulation patterns without introducing excessive errors into the trajectory estimates that may arise over longer time scales.

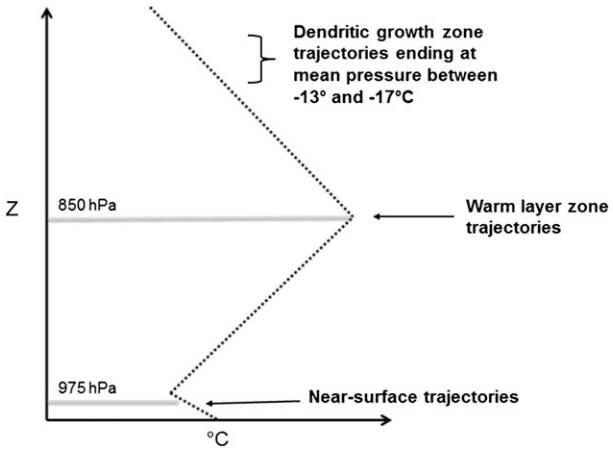

FIG. 3. Schematic of the vertical temperature profile and the three critical levels from which back trajectories were computed. The dotted line represents the environmental lapse rate.

Trajectories associated with the near-surface level reveal the circulation within the low-level cold wedge that is typically present during winter precipitation in the region. The decision to use the 975-hPa level was based on examination of modeled soundings using the EDAS output, which showed good agreement with the observed soundings at that level (not shown; see Fuhrmann 2011). The 850-hPa level was chosen to represent the warm layer zone because it is a standard pressure level used routinely to forecast precipitation type. Above (below) freezing temperatures in the warm layer zone at 850 hPa, as indicated by the modeled and observed soundings (not shown), were associated with ice storms (snowstorms). Determining the processes and upstream features that contribute to these warm layer zone temperatures is a major goal of this study. Finally, trajectories associated with the dendritic growth zone reveal the properties of the air associated with ice crystal formation growth. It has been noted that ice crystal growth in the dendritic range, when combined with sufficient moisture and upward vertical motion, can lead to heavy snowfall (Auer and White 1982; Perry 2006). Therefore, trajectories calculated in this layer (from 600 to 450 hPa) can aid in determining the processes and upstream features that contribute to the formation of precipitation in the wintertime atmosphere over central North Carolina.

The hourly latitude and longitude associated with each back trajectory were used to develop composite trajectories for snowstorms and ice storms at each of the three critical levels. Composite trajectories were created by calculating the median coordinates among all events at 1-h trajectory segments. To illustrate the representativeness of the composite trajectories, a trajectory envelope was created around each composite trajectory. Similar to a climate envelope, the trajectory envelope illustrates the range of possible trajectories from the sample of storms. Composite trajectories and trajectory envelopes were also constructed for the vertical trajectory coordinates as well as several meteorological variables along each trajectory, including temperature (°C), moisture (mixing ratio; g kg^{-1}), vertical velocity (cm s^{-1}), and potential temperature (θ; K). Only composite trajectories of vertical coordinates and meteorological variables are presented in this study due to similarities in the trajectory characteristics among the individual storms and to facilitate comparisons between the different vertical levels. In general, the trajectory characteristics were most similar among individual storms at T-0 h (ending time) and exhibited increasing variability to T-72 h (starting time). For instance, the variability in moisture content in the warm layer zone among all events ranged from approximately 7% at T-0 h to nearly 90% at T-72 h, while the corresponding variability in θ ranged from 1 to 8 K over the 72-h trajectory period. There was also greater variability in the trajectory characteristics among the snowstorms than among the ice storms. The full range of trajectory envelopes can be found in Fuhrmann (2011).

Additionally, a procedure was devised to calculate the amount of adiabatic warming and cooling relative to the amount of diabatic warming and cooling for air parcels traveling along each trajectory segment. As air parcels move vertically through the atmosphere, they warm and cool dry adiabatically at a fixed rate of 9.8°C $(1000\ m)^{-1}$ (i.e., the dry-adiabatic lapse rate, DALR). If the change in air parcel temperature from one hour to the next along a given trajectory matches the DALR, then the parcel is assumed to have warmed or cooled adiabatically with no contributions from diabatic processes. If the change in temperature does not match, then the residual is considered to be a result of diabatic processes. For example, if an air parcel rises 0.2 km, it should cool by 2°C according to the DALR. However, if the parcel is observed to warm 4°C, then a net diabatic warming of 6°C is said to have occurred. Although the specific processes contributing to diabatic warming and cooling are not explicitly diagnosed, it is assumed that a large proportion of the diabatic temperature change is due to latent heating and cooling.

To distinguish between the trajectories at locations with different precipitation types and intensities in a given event, a set of comparative back trajectories were calculated for two of the events (one snowstorm and one ice storm). These comparative trajectories were calculated to determine which of the ingredients (i.e., temperature, moisture, lift) and processes (i.e., adiabatic

or diabatic) best distinguishes between different precipitation types and intensities in a given event. These comparative trajectories are not meant to be representative of all snowstorms and ice storms. Instead, they are presented here to illustrate the utility of the trajectory approach in forecasting patterns of precipitation type and intensity across a particular forecast area.

3. Snowstorms

Figure 4 illustrates the horizontal component of the 72-h back trajectories associated with the eight snowstorms. The near-surface trajectory originated over the Great Lakes at T-72 h and exhibited an anticyclonic curvature as it approached central North Carolina. Examination of corresponding surface weather maps revealed that the near-surface trajectory originated along the eastern periphery of a surface anticyclone centered over the Great Lakes and central Canada (not shown). Air parcels terminating in the warm layer zone (WLZ) at T-0 h also originated over the Great Lakes, but traveled southeastward to a point off of the mid-Atlantic coast before shifting course to the southwest toward central North Carolina. This sharp southwestward turn corresponded with an intensifying surface cyclone moving out of the Gulf of Mexico and up the East Coast (not shown). While the near-surface and WLZ trajectories were similar across all the snowstorms, examination of trajectories terminating in the dendritic growth zone (DGZ) revealed two distinct paths and source regions. In four of the eight snowstorms, the trajectory terminating in the DGZ originated over the eastern Great Lakes and traveled anticyclonically across the northeast United States (hereafter referred to as the DGZ-anticyclonic trajectory; Fig. 4). These air parcels continued traveling southward over the Atlantic Ocean before recurving toward central North Carolina. In the other four snowstorms, the air associated with the DGZ originated over the Caribbean Sea and exhibited a subtle cyclonic curvature as it approached central North Carolina (hereafter referred to as the DGZ-cyclonic trajectory; Fig. 4). These diverging paths did not show any relationship with the height of the DGZ.

The corresponding mean vertical component of the 72-h back trajectories is illustrated in Fig. 5a. The near-surface air parcel originated at approximately 1 km above ground level and gradually descended over the course of the trajectory along the periphery of the anticyclone. The WLZ trajectory originated at approximately 2.5 km and descended to near 1 km near the Delmarva Peninsula between T-48 and T-36 h (see Fig. 4), with a subtle rise in altitude over the last 6 h of the trajectory. Both DGZ trajectories originated between 1 and 1.5 km and descended to below 1 km at T-38 h. The DGZ-cyclonic trajectory reached a minimum height of approximately 0.5 km at T-30 h while the DGZ-anticyclonic trajectory remained just below 1 km. At T-12 h, both DGZ trajectories rose abruptly from near 1 km to their terminating altitude near 5 km, indicating the presence of strong upward vertical motion associated with a well-developed surface cyclone.

Figure 5b illustrates the air temperature along each trajectory. The near-surface air parcels exhibited a gradual warming from −12° to −3°C over the course of the trajectory, likely due to adiabatic or compressional warming along the periphery of a surface anticyclone. The WLZ trajectory also revealed a warming of air parcels from T-72 to T-36 h, followed by a gradual cooling of air parcels to −5°C as they entered central North Carolina. A possible mechanism for this cooling is explored later within the context of diabatic processes. Air parcels associated with the DGZ-anticyclonic trajectory also warmed over much of the trajectory period before abruptly cooling over the final 12 h of the trajectory period, likely due to adiabatic expansion resulting from strong upward vertical motion. In contrast, air parcels associated with the DGZ-cyclonic trajectory remained remarkably warm (near 15°C) for most of the trajectory before abruptly cooling as they entered the DGZ.

Moisture composites were calculated along each trajectory at each critical vertical pressure level (Fig. 5c). The moisture content of the near-surface air parcels increased slightly throughout most of the trajectory period (1–2 g kg^{-1}), with an increase from 2 to 3 g kg^{-1} over the last 6 h of the trajectory. This short-term increase may be due to virga or evaporating and sublimating precipitation. The moisture content of the WLZ air parcels exhibited a gradual increase of 1–3 g kg^{-1} from T-72 to T-36 h, and then exhibited little change over the remainder of the trajectory. In contrast, the moisture content of the DGZ trajectories revealed well-defined evaporation–precipitation cycles. These cycles are identified by the initial rise in moisture content resulting from surface evaporative fluxes (e.g., from an upstream body of water) followed by a decrease in moisture resulting from condensation and deposition (James et al. 2004). Though the rate increase in moisture content over the first part of the cycle (from T-72 to T-12 h) is similar between the DGZ trajectory types, the DGZ-cyclonic trajectory exhibited much larger overall moisture contents (4.5–8.2 g kg^{-1}) than did the DGZ-anticyclonic trajectory (1.8–5.8 g kg^{-1}) due to its origin over the warm waters of the Caribbean Sea. Moreover, the rate of decrease in moisture content (i.e., the rate of condensation and deposition) was much greater with DGZ-cyclonic trajectories. As a result, snowstorms with DGZ-cyclonic

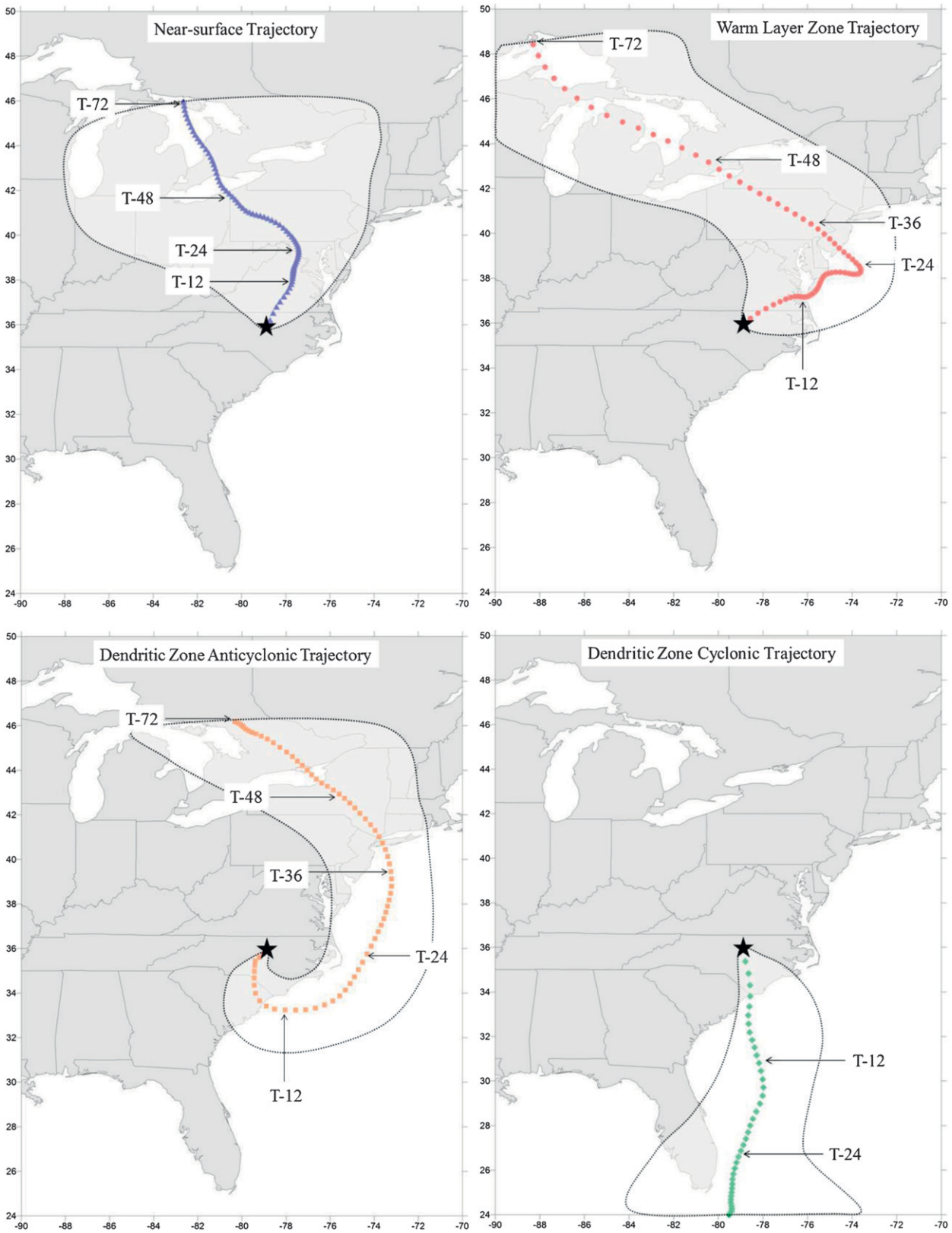

FIG. 4. Horizontal trajectory composites and trajectory envelopes of air parcels terminating at (from top to bottom) the near surface, WLZ, and the dendritic growth zone in the region of heavy snowfall. Stars indicate the mean trajectory ending point (T-0 h). The horizontal position of the composite trajectory at several different trajectory periods is indicated to facilitate comparisons between trajectory locations and meteorological variables.

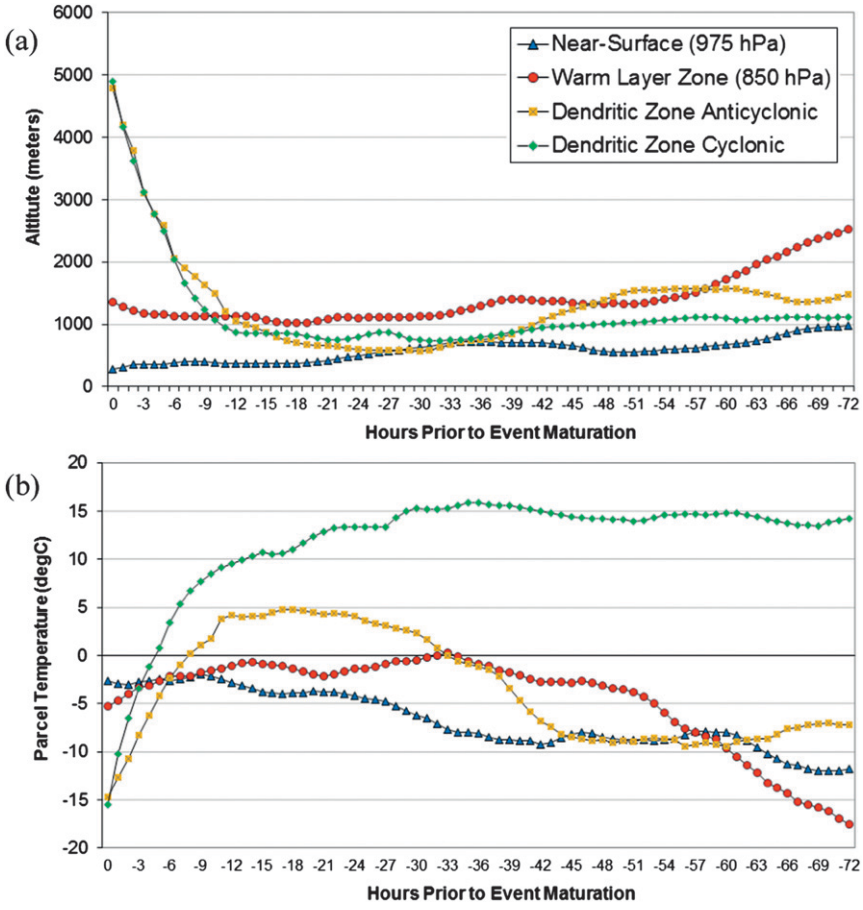

FIG. 5. Composite trajectories of (a) height (m), (b) temperature (°C), (c) moisture (g kg^{-1}), and (d) potential temperature (K) for air parcels terminating at the near surface, WLZ, and the dendritic growth zone in the region of heavy snowfall.

trajectories exhibited higher maximum precipitation rates (0.05–0.12 in. h^{-1}) than snowstorms with DGZ-anticyclonic trajectories (0.04–0.07 in. h^{-1}). The reduction in moisture resulting from condensation and deposition in the presence of strong upward vertical velocity indicates that much of the moisture supply was converted into precipitation (James et al. 2004).

To determine whether diabatic processes were occurring along each trajectory, the potential temperature (θ) of the air parcels was calculated. Figure 5d illustrates the composite θ values along the trajectories from each critical vertical pressure level. The θ values along both the near-surface and WLZ trajectories were nearly constant over the 72-h trajectory period. In contrast, the DGZ-anticyclonic and DGZ-cyclonic trajectories exhibited increases in θ over the final 10 h of the trajectory from 277 to 295 K and from 294 to 308 K, respectively. The increase in θ corresponded with large reductions in moisture content along the DGZ trajectories (Fig. 5c). It is likely that the latent heat released due to condensation and deposition resulted in strong diabatic heating, which is reflected by the increase in θ along the trajectories. Therefore, the increase in θ suggests a diabatic contribution to the DGZ trajectories from condensation and deposition.

Figure 6 shows the net diabatic contribution to air parcel temperatures summed across the entire 72-h trajectory period and reveals that diabatic processes contributed on average between 9° and 13°C of warming to the DGZ trajectories. In other words, in the absence of diabatic processes, the resulting air parcel temperature by the end of the trajectory would have been 9°C–13°C cooler than observed at the beginning of the trajectory. By comparison, diabatic processes contributed less than 4°C of warming to the near-surface trajectories. Interestingly, several snowstorms exhibited net diabatic cooling (<0°C) of air parcels along the WLZ trajectory. This was likely due to latent heat absorption from evaporation–sublimation, as the moisture content steadily increased along the trajectory (Fig. 5c).

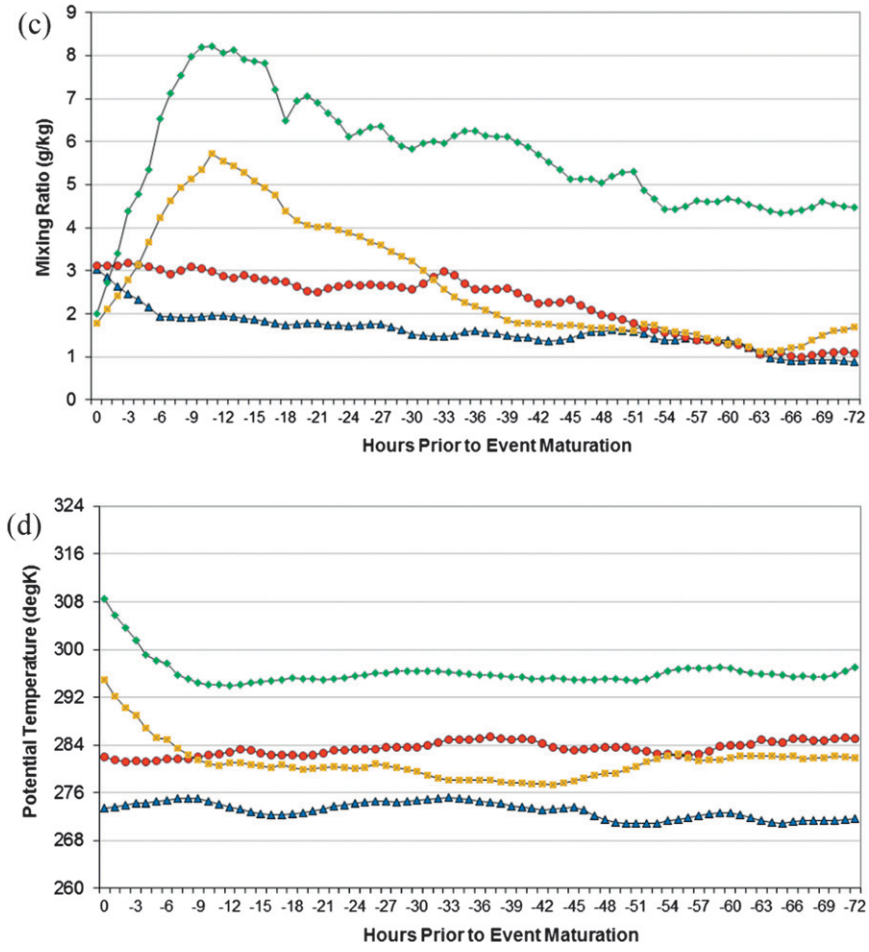

FIG. 5. (*Continued*)

Because the WLZ temperature is frequently used to discriminate between snow and freezing rain–sleet scenarios, it is important to diagnose the processes that contribute to the temperature at this level. Figure 7 illustrates the observed air parcel temperature and the adiabatic air parcel temperature (i.e., the temperature of the air parcel with no diabatic contributions) at 6-h segments along the trajectory. From T-72 to T-36 h, the observed temperature was slightly higher on average than the adiabatic temperature, which indicates the occurrence of diabatic warming. The large variation in observed temperature across the snowstorm cases early in the trajectory period may be tied to variations in the temperature of the upstream air mass over the Great Lakes. In contrast, the observed temperature over the final 36 h of the trajectory was slightly lower than the adiabatic temperature. In particular, the range in adiabatic temperature among the eight snowstorms over the final 6 h of the trajectory was from −7° to 3°C. This indicates that in some cases the observed temperature would have been above freezing at the time of precipitation in the absence of diabatic cooling. With a WLZ temperature of 3°C, it is conceivable that at least partial melting of precipitation would have occurred, resulting in either wet snow, sleet, or freezing rain. These results indicate the importance of accurately diagnosing the amount of diabatic cooling due to latent heat absorption from evaporation when making a precipitation-type forecast in the region.

To distinguish between trajectories at locations and times with different precipitation types and intensities in a given storm, a set of comparative trajectories was calculated for the snowstorm of 24–25 January 2000. This event was one of the most remarkable winter storms ever recorded across central North Carolina, both for the record snowfall amounts that were recorded and for the failure of most numerical weather prediction models to adequately forecast the evolution of the storm and the resulting precipitation (Brennan and Lackmann 2005). It was selected for further analysis because of the

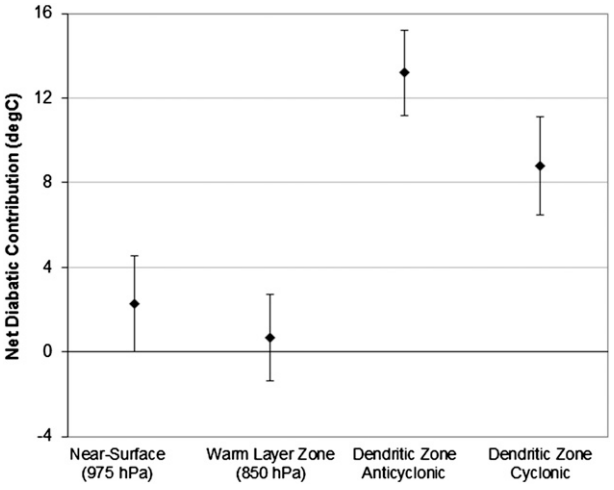

FIG. 6. Net diabatic contribution to air parcel temperature (°C) at each critical level in the region of heavy snowfall. Range bars indicate the maximum and minimum values among all eight snowstorms.

great disparity in snowfall totals and precipitation rates across the study area. Snowfall amounts across the Raleigh CWA ranged from approximately 2 in. (5.1 cm) in the western- and easternmost areas of the CWA to as much as 22 in. (55.9 cm) across the central portion of the CWA (see Fuhrmann 2011, Fig. A1). Raleigh-Durham, North Carolina (RDU), recorded 20.3 in. (51.6 cm), which is the most snowfall from a single storm in a station record extending back to 1944. By comparison, Winston-Salem, North Carolina (INT), located 130 km west of RDU (see Fig. 2), recorded only 2.3 in. (5.8 cm) of snowfall from the event, while Rocky Mount, North Carolina, located 94 km east of RDU, recorded 6.8 in. (17.3 cm) of snow. The disparity in snowfall totals across the CWA is further revealed in the hourly precipitation totals from the storm (not shown). For example, RDU recorded 5 in. (12.7 cm) of snow in 1 h (ending at 0600 UTC 25 January), more than double the amount of precipitation observed at RWI, while INT recorded just a trace of precipitation.

Examination of the corresponding back trajectories provides some insight into the disparity in the precipitation totals. Of particular importance are the differences in the space–time character and meteorological properties of the DGZ trajectories. At RDU and RWI, the DGZ trajectories originated near the Caribbean Sea and traveled northward over the Gulf Stream, then turned cyclonically, and ascended into the region of precipitation (Figs. 8a,b). These trajectories spent considerable time over warm ocean waters and revealed well-defined evaporation–precipitation cycles (Fig. 9). However, the maximum moisture content of the DGZ air at RDU was nearly 4 g kg^{-1} greater than at RWI, indicating that there was more moisture available for precipitation at RDU compared to RWI.

In contrast, the DGZ trajectory at INT originated near the southern tip of Florida and turned anticyclonically across northern Florida and Georgia before turning

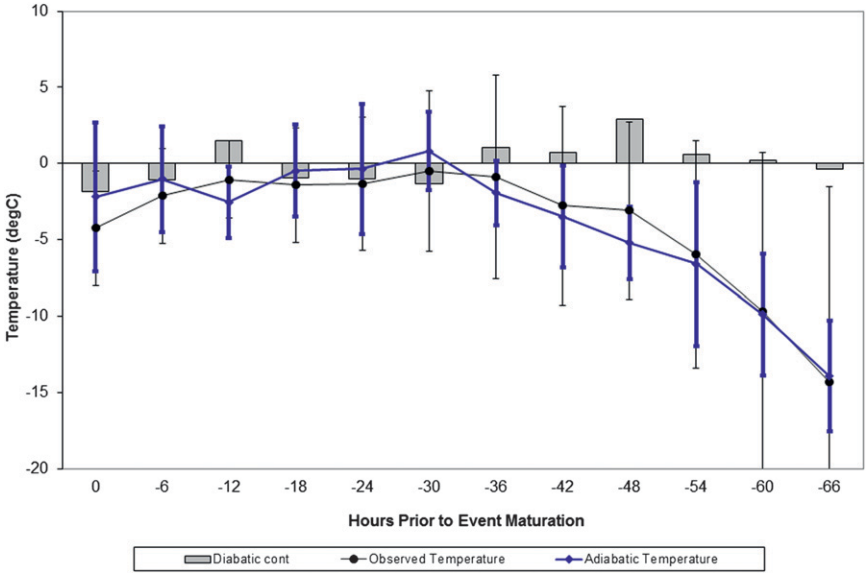

FIG. 7. Composite WLZ trajectories of observed air parcel temperature (°C) (black line), adiabatic temperature (thick blue line), and diabatic contribution (gray bars) in the region of heavy snowfall at 6-h trajectory segments. Range bars indicate the maximum and minimum values among all eight snowstorms.

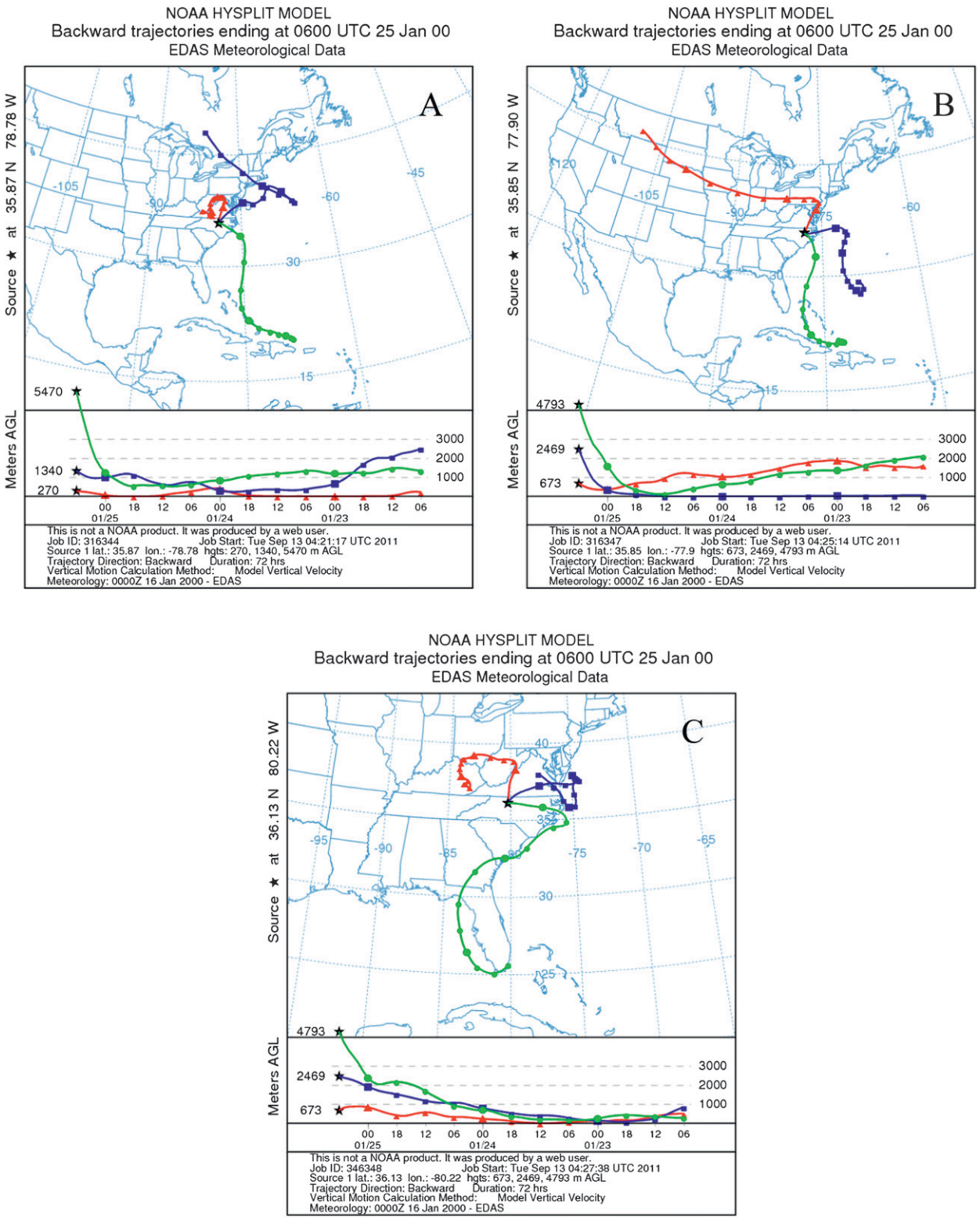

FIG. 8. Horizontal and vertical trajectories for 0600 UTC 25 Jan 2000 terminating at the near-surface level (red trajectories), WLZ (blue trajectories), and DGZ (green trajectories) at (a) RDU, (b), RWI, and (c) INT. Vertical trajectories (m) are shown at the bottom of each panel.

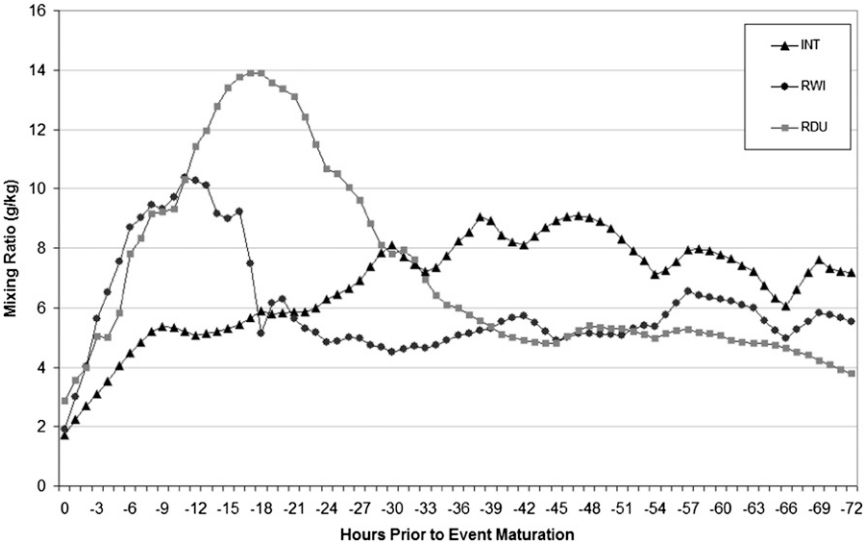

FIG. 9. Air parcel trajectories of moisture content (g kg^{-1}) for 0600 UTC 25 Jan 2000 terminating in the DGZ at RDU, RWI, and INT.

cyclonically up the Carolina coastline and into the region of precipitation (Fig. 8c). The moisture content along the INT trajectory exhibited a gradual decline from T-72 to T-36 h, with only half the moisture available for precipitation over the last 6 h of the trajectory compared to RDU and RWI (Fig. 9). The reduction in moisture seen in the INT trajectory coincided with the air parcel moving out from over the Gulf of Mexico and crossing into southern Georgia. Moreover, over the final 6 h of the DGZ trajectories, the air parcels terminating at INT ascended at a slower rate than at RWI and RDU. The mean vertical velocity was 17 cm s^{-1} at RDU, versus 13 cm s^{-1} at RWI and 9 cm s^{-1} at INT. The results of the trajectory calculations therefore suggest that a combination of greater moisture content, likely due to increased latent heat fluxes, and greater upward vertical velocity contributed to higher precipitation rates at RDU in the 24–25 January 2000 event. Although this event was poorly forecasted by several numerical weather prediction models, the results of the trajectory analyses are consistent with surface and upper-air observations of the event at the time of heaviest precipitation at RDU (Buzzia and Chessa 2002; Brennan and Lackmann 2005).

4. Ice storms

Figure 10 illustrates the horizontal component of the 72-h back trajectories associated with the seven ice storms. The near-surface trajectory originated over the Great Lakes and exhibited anticyclonic curvature as it approached central North Carolina. This trajectory is qualitatively similar to the near-surface trajectory and composite synoptic pattern observed in the snowstorm cases and traces the path of air parcels associated with cold-air damming (Richwien 1980; Bell and Bosart 1988) (see Fig. 4). Air parcels terminating in the WLZ also originated over the Great Lakes region, but continued traveling southeastward before turning anticyclonically over the Atlantic Ocean in the vicinity of the Gulf Stream and approaching central North Carolina from the southeast. This is in contrast to the WLZ trajectory observed in the snowstorm cases, which approached central North Carolina from the northeast and traveled over presumably cooler ocean waters at an altitude around 1 km. As in the snowstorm cases, the near-surface and WLZ trajectories were similar across all the ice storms, while the DGZ trajectories exhibited two distinct paths and source regions. In four of the seven ice storms, the trajectory terminating in the DGZ originated over the Gulf of Mexico and exhibited general anticyclonic curvature as it approached central North Carolina (hereafter referred to as the DGZ-Gulf trajectory). These trajectories were associated with a primary surface cyclone located to the southwest and a secondary cyclone off of the Southeast coast (not shown). In the other three ice storms, the air associated with the DGZ was of eastern Pacific origin and exhibited subtle cyclonic curvature as it approached central North Carolina (hereafter referred to as the DGZ-Pacific trajectory). These trajectories were associated with a relatively weaker surface cyclone located to the southwest and no secondary cyclone (not shown). As in the snowstorm cases, these diverging paths did not show any relationship with the height of the DGZ.

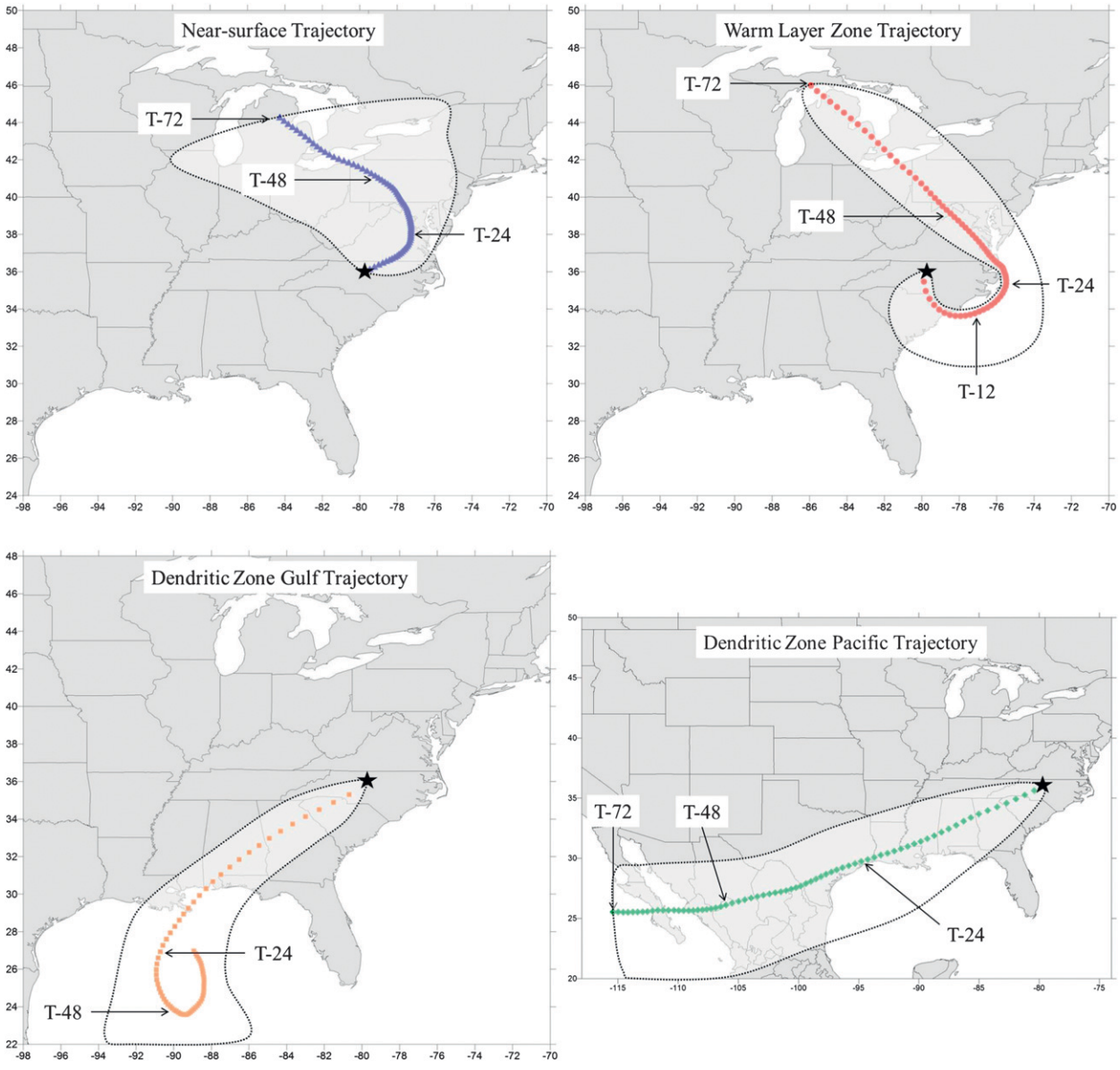

FIG. 10. As in Fig. 4, but in the region of heavy freezing precipitation.

As in the snowstorm cases, the near-surface air parcel originated at approximately 1 km above ground level and gradually descended over the course of the trajectory (Fig. 11a). The WLZ trajectory originated at approximately 1.5 km and descended to below 0.2 km off of the North Carolina coast before rising again to 1.5 km over the last 15 h of the trajectory. The DGZ-Gulf trajectory also originated at approximately 1.5 km and remained at the same altitude from T-72 to T-24 h before rising to its terminating altitude near 5.5 km. In contrast, the DGZ-Pacific trajectory originated near 5 km and descended to a minimum height of 3.5 km at T-30 h. Beginning at T-6 h, the DGZ-Pacific trajectory rose from 3.7 km to its terminating altitude of 5.5 km. These DGZ trajectories indicate more gradual lifting compared to the snowstorm cases, which may be tied to quasigeostrophic ascent resulting from warm advection and differential positive vorticity advection (Robbins and Cortinas 2002). Indeed, synoptic analyses at 850 and 500 hPa revealed short-wave troughs located over the central Great Plains and therefore an increased southerly component to the large-scale flow over the Southeast relative to the snowstorm cases (not shown).

Similar to the snowstorm cases, the near-surface air parcels exhibited a gradual warming over the course of the trajectory (Fig. 11b). However, the starting temperature

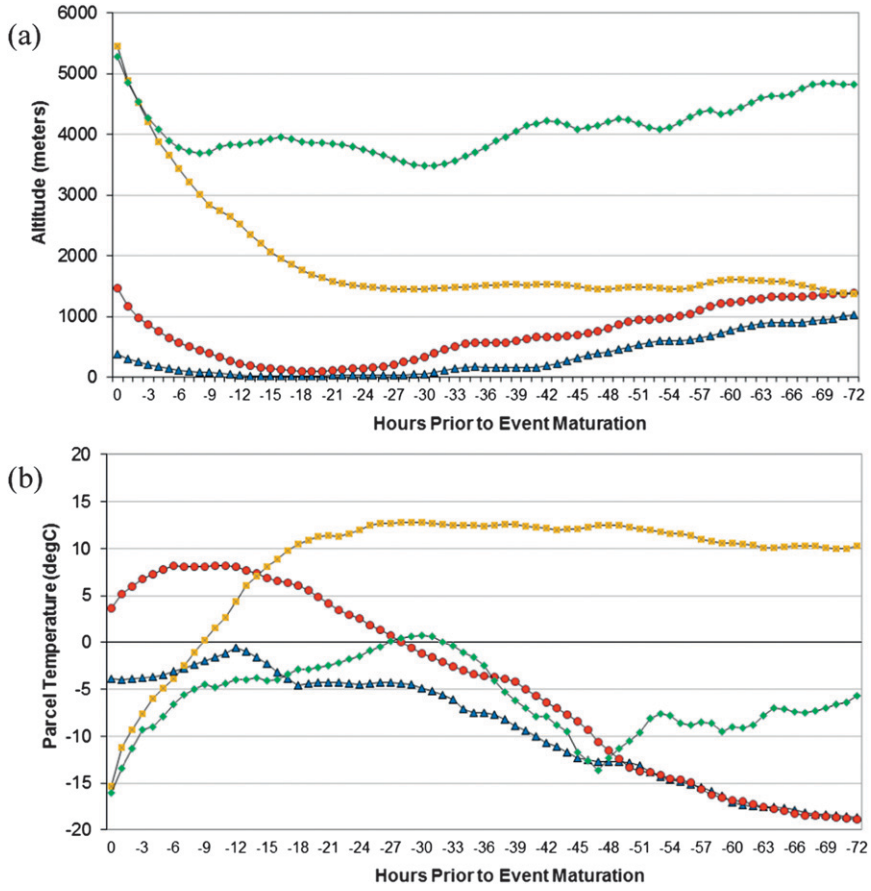

FIG. 11. As in Fig. 5, but in the region of heavy freezing precipitation.

was colder in the ice storm composite (−18°C compared to −12°C) and exhibited a cooling from −1° to −4°C over the last 12 h of the trajectory. The WLZ trajectory revealed a gradual warming of air parcels from T-72 to T-30 h. However, unlike the snowstorm composite, the WLZ trajectory in the ice storm composite continued to warm to a maximum temperature of 8°C at T-12 h. A possible mechanism for this warming is explored below within the context of diabatic processes. This was followed by a slight cooling of air parcels to 4°C as they entered the elevated warm layer over central North Carolina. Temperatures associated with the DGZ-Pacific trajectory were highly variable from T-72 to T-48 h before warming to 0°C at T-30 h. This was followed by a gradual cooling of air parcels as they entered the DGZ. In contrast, air parcels associated with the DGZ-Gulf trajectory remained remarkably warm (near 12°C) for most of the trajectory before abruptly cooling as they entered the DGZ. This temperature trajectory is very similar to the trajectory observed in the DGZ-cyclonic snowstorm composite.

As in the snowstorm cases, the moisture content of the near-surface air parcel gradually increased throughout most of the trajectory period (1–2 g kg^{-1}) and then increased from 2 to 3 g kg^{-1} over the last 10 h of the trajectory (Fig. 11c). The WLZ trajectory exhibited a small increase in moisture (0.5–1.0 g kg^{-1}) from T-72 to T-36 h, but then exhibited an abrupt increase in moisture (1.0–6.5 g kg^{-1}) from T-32 to T-4 h. This increase was followed by a small decrease in moisture content over the last 4 h of the trajectory. The abrupt increase in moisture corresponded to the position of the WLZ trajectory off of the North Carolina coast from T-30 to T-6 h at an altitude of less than 0.5 km (see Fig. 10). It is suggested that large evaporative fluxes from the ocean surface contributed to the moisture composite along the WLZ trajectory as it approached the region of heavy freezing precipitation.

In contrast, the DGZ-Pacific trajectory exhibited a relatively weak evaporation–precipitation cycle as moisture contents gradually increased from 0.5 to 3.6 g kg^{-1} over most of the trajectory period. The decrease in moisture over the last 6 h of the trajectory was markedly lower in comparison to the DGZ trajectories in the snowstorm composites (i.e., lower rates of condensation

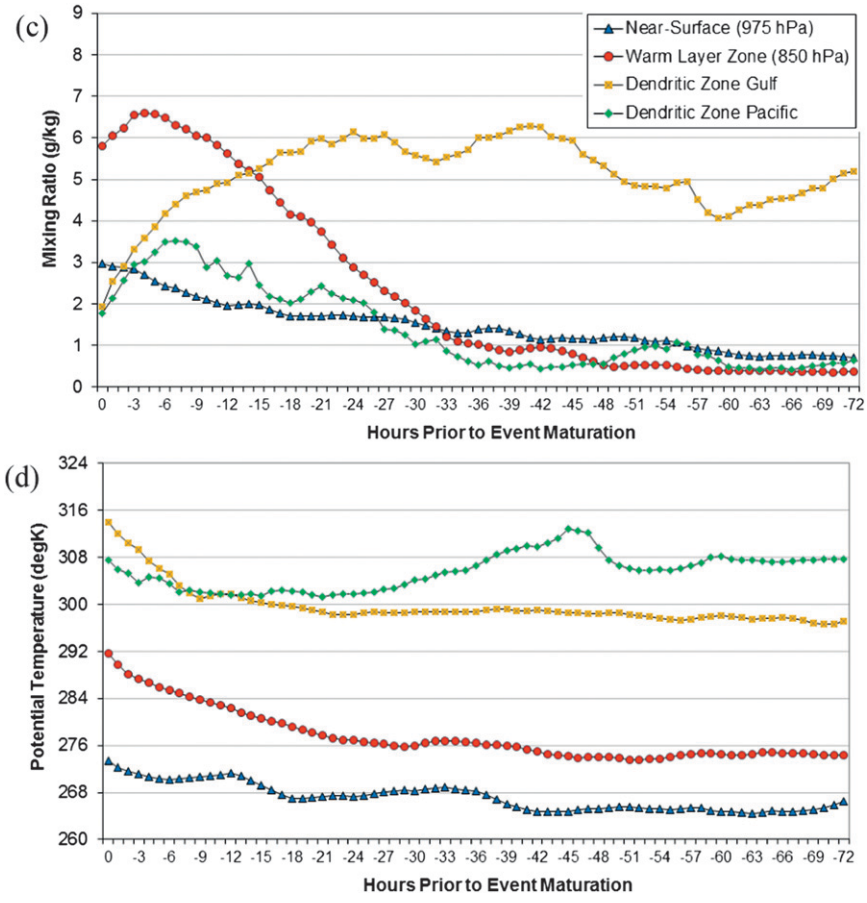

FIG. 11. (*Continued*)

and deposition). In contrast, the DGZ-Gulf trajectory exhibited much larger overall moisture contents (as much as 6.2 g kg^{-1}) than did the DGZ-Pacific trajectory. Moreover, the rate decrease in moisture content was much greater with the DGZ-Gulf trajectory, implying higher rates of condensation and deposition. Indeed, ice storms with DGZ-Gulf trajectories exhibited higher maximum precipitation rates (0.11–0.22 in. h^{-1}) than ice storms with DGZ-Pacific trajectories (0.03–0.09 in. h^{-1}).

Composite θ values along each trajectory are illustrated in Fig. 11d. As in the snowstorm cases, the near-surface trajectory exhibited very little change in θ over the trajectory period. In contrast, the WLZ trajectory exhibited an increase in θ over the final 30 h of the trajectory from 276 to 292 K. The increase in θ corresponded with a large increase in moisture content along the trajectory (Fig. 11c). In this case, as relatively cold, dry air initially associated with the WLZ trajectory flows out over the warmer Gulf Stream waters, it likely induces high fluxes of sensible and latent heat from the ocean to the atmosphere (Bane and Osgood 1989). The increases in sensible and latent heat fluxes are therefore reflected in the increases in air parcel temperature and θ along the WLZ trajectories. The θ values along the DGZ-Gulf trajectory were nearly constant over most of the 72-h trajectory period, while the DGZ-Pacific trajectory exhibited a decrease in θ beginning around T-48 h. Both DGZ trajectories exhibited increases in θ over the last 6 h of the trajectory in response to diabatic heating from condensation and deposition.

Unlike the snowstorm cases, diabatic processes contributed most significantly to the warming of the WLZ trajectory temperature (Fig. 12). Over the 72-h trajectory period, diabatic processes contributed between 18° and 22°C of warming to the WLZ trajectory (i.e., in the absence of diabatic processes, the air parcel temperature by the end of the trajectory would have been 18°–22°C cooler than observed at the beginning of the trajectory). By comparison, diabatic processes contributed approximately 10°C of warming to the near-surface trajectory and 12°C of warming to the DGZ-Gulf trajectory over the 72-h trajectory period. In contrast, the DGZ-Pacific trajectory received negligible contributions from diabatic processes over the trajectory period. Examination

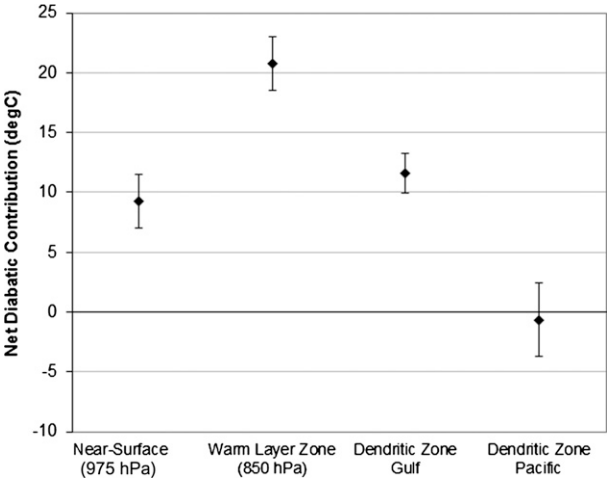

FIG. 12. As in Fig. 6, but in the region of heavy freezing precipitation.

of the observed air parcel temperature and adiabatic air parcel temperature along the WLZ trajectory indicated negligible contributions from diabatic processes from T-72 to T-48 h, with significant diabatic warming over the final 48 h of the trajectory (Fig. 13). In particular, while the observed temperature over the last 6 h of the trajectory was 4°C, the adiabatic temperature was −2°C. This indicates that the observed temperature would have been *below* freezing at the time of precipitation in the absence of diabatic warming. With a WLZ below freezing, it is likely that snow would have been observed instead of freezing rain (assuming the near-surface temperature profile was also supportive of snow).

As in the previous section on snowstorms, a set of comparative trajectories was calculated for one of the seven ice storms. The ice storm of 4–5 December 2002 was a major event that initially struck the southern plains before moving through the Southeast and mid-Atlantic regions. Duke Energy referred to the storm as ''the worst'' in their 100-yr history, as 1.5 million customers lost power across North and South Carolina (Fuhrmann et al. 2009). Freezing rain totals across the Raleigh CWA ranged from 0.12 in. (0.3 cm) in the easternmost areas of the CWA to over 1.5 in. (3.8 cm) across the central portion of the CWA (see Fuhrmann 2011, Fig. A10). A broad swath of at least 0.5 in. (1.3 cm) of freezing rain extended from southwest to northeast across central North Carolina and included the cities of Charlotte, Greensboro (GSO), and Raleigh-Durham. However, there was much variation in the freezing totals within this area. For example, RDU recorded 1.16 in. (2.9 cm) of freezing rain from the event, with nearly half occurring in a 3-h period from 0400 to 0600 UTC 5 December (not shown). In contrast, GSO, located just 100 km to the west, recorded 0.5 in. (1.3 cm) of freezing rain from the event. Moreover, during the 3-h period of heavy freezing rain at RDU, only 0.06 in. (0.15 cm) was recorded at GSO. This storm was selected for further analysis because of the significant variability in freezing rain totals and precipitation rates across the study area.

Examination of the corresponding back trajectories provides insight into the disparity in precipitation totals between RDU and GSO. Of particular importance are the differences in the space–time character and meteorological properties of the WLZ and DGZ trajectories.

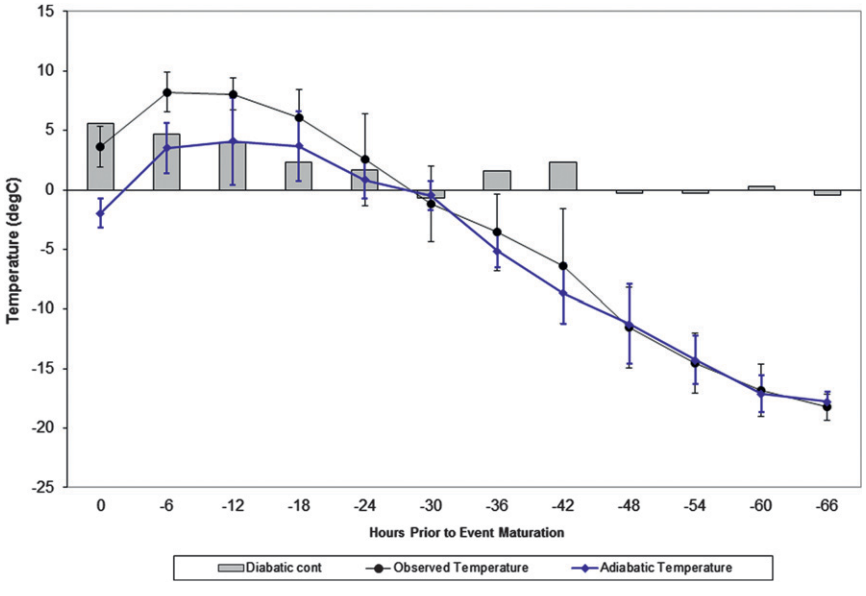

FIG. 13. As in Fig. 7, but in the region of heavy freezing precipitation.

At RDU, the DGZ trajectory originated over the western Gulf of Mexico at an altitude of 3.7 km and traveled northeast (i.e., cyclonically) toward central North Carolina (Fig. 14a). Air parcels remained above 3.5 km for most of the trajectory period before ascending into the DGZ at RDU. By comparison, the DGZ trajectory at GSO originated over the eastern Pacific Ocean near the coast of Mexico and took a similar path to the one observed at RDU (Fig. 14b). Both DGZ trajectories exhibited similar vertical velocities over the last 6 h of the trajectory (7.8 cm s^{-1}), while the DGZ trajectory at GSO remained at a slightly higher altitude (4 km) for the majority of the trajectory period. Interestingly, despite the small difference in trajectory heights, the maximum moisture content of the DGZ trajectory at GSO was markedly lower (4.5 g kg^{-1}) than that observed in the DGZ trajectory at RDU (7.2 g kg^{-1}) (Fig. 15a). The difference in maximum moisture contents over the evaporation–precipitation cycle likely contributed to the higher rate of freezing rain at RDU.

Inspection of the moisture contents along the WLZ trajectories revealed another possible contributor to the higher freezing rain rate at RDU. Both WLZ trajectories exhibited a rapid rise in moisture content beginning at T-24 h as they traveled over the Atlantic Ocean (Fig. 15b). Additionally, air parcels in both WLZ trajectories ascended at a rate of 4.8 cm s^{-1} over the last 6 h of the trajectory. However, the RDU trajectory revealed a decrease in moisture content of approximately 2 g kg^{-1} over the last 4 h of the trajectory while moisture contents continued to rise along the WLZ trajectory at GSO (Fig. 15b). The decrease in moisture content in the presence of upward vertical motion indicates that some of the moisture in the WLZ was converted into precipitation at RDU. These results suggest that the WLZ trajectory was an important contributor to the enhanced precipitation rates at RDU.

5. Discussion and conclusions

In this study, air parcel trajectory analyses were found to be useful in assessing the evolution of the ingredients and physical processes that come together to produce a winter storm. This study also demonstrated the potential utility of trajectory analyses in an operational forecast setting through a diagnosis of upstream meteorological conditions, thereby providing insight into the physical processes contributing to an event as well as guidance on forecast model output. As shown for a sample of winter storms that affected central North Carolina, the details of the back-trajectory motions and air parcel characteristics often have a significant influence on the intensity of the precipitation as well as the precipitation type (e.g., snow versus freezing rain). Nevertheless, examination of a larger sample of events of varying intensities is needed to establish climatologically robust connections between the trajectory motions, their characteristics, and their source regions.

One of the major goals of this research was to determine the processes and upstream features that contribute to WLZ temperatures, as winter precipitation forecasts involving frozen or freezing precipitation require an accurate diagnosis of temperatures in the WLZ. The temperature of the WLZ was found to be related to the amount of diabatic warming and cooling resulting from sensible and latent heat fluxes over the course of the trajectory period. In the snowstorm cases, the observed temperature and adiabatic temperature along the WLZ trajectory showed a net diabatic cooling over the final 6 h of the trajectory. The exact process responsible for this cooling was not determined. One possibility is latent heat absorption due to sublimation of falling snowflakes, which can counteract the warming due to adiabatic processes (Bell and Bosart 1988; Market et al. 2006). Previous studies have also noted that melting of snowflakes can aid in lowering the freezing level so that snow can reach the surface, particularly in regions of heavy precipitation (Field and Stewart 1994; Kain et al. 2000). However, the increase in moisture along the WLZ trajectory suggests that evaporation–sublimation was the more likely process, though latent heat absorption due to melting may have been occurring below this level (i.e., below 850 hPa). Examination of multiple atmospheric levels may reveal the full range of processes contributing to the vertical temperature profile and resulting precipitation characteristics. Future work should also consider use of the moist-adiabatic lapse rate to gain further insights into the role of diabatic processes on the resulting air parcel temperatures.

In contrast to the snowstorm cases, the WLZ trajectory in the ice storm cases likely descended within the marine atmospheric boundary layer (MABL) (<0.2 km) and therefore induced high fluxes of sensible and latent heat from the ocean to the atmosphere (Bane and Osgood 1989). Examination of the observed temperature and adiabatic temperature along the WLZ trajectory revealed that air in the WLZ would have been below freezing in the absence of diabatic warming. Therefore, sensible and latent heat fluxes within the MABL off of the Carolina coast may be direct contributors to the occurrence of ice storms in central North Carolina. The basis for this conclusion is provided by Gyakum and Roebber (2001). Their study of the major ice storm of 1998 over southeast Canada revealed that air parcels connected with the heavy freezing rain spent considerable time in the Atlantic MABL where sensible and

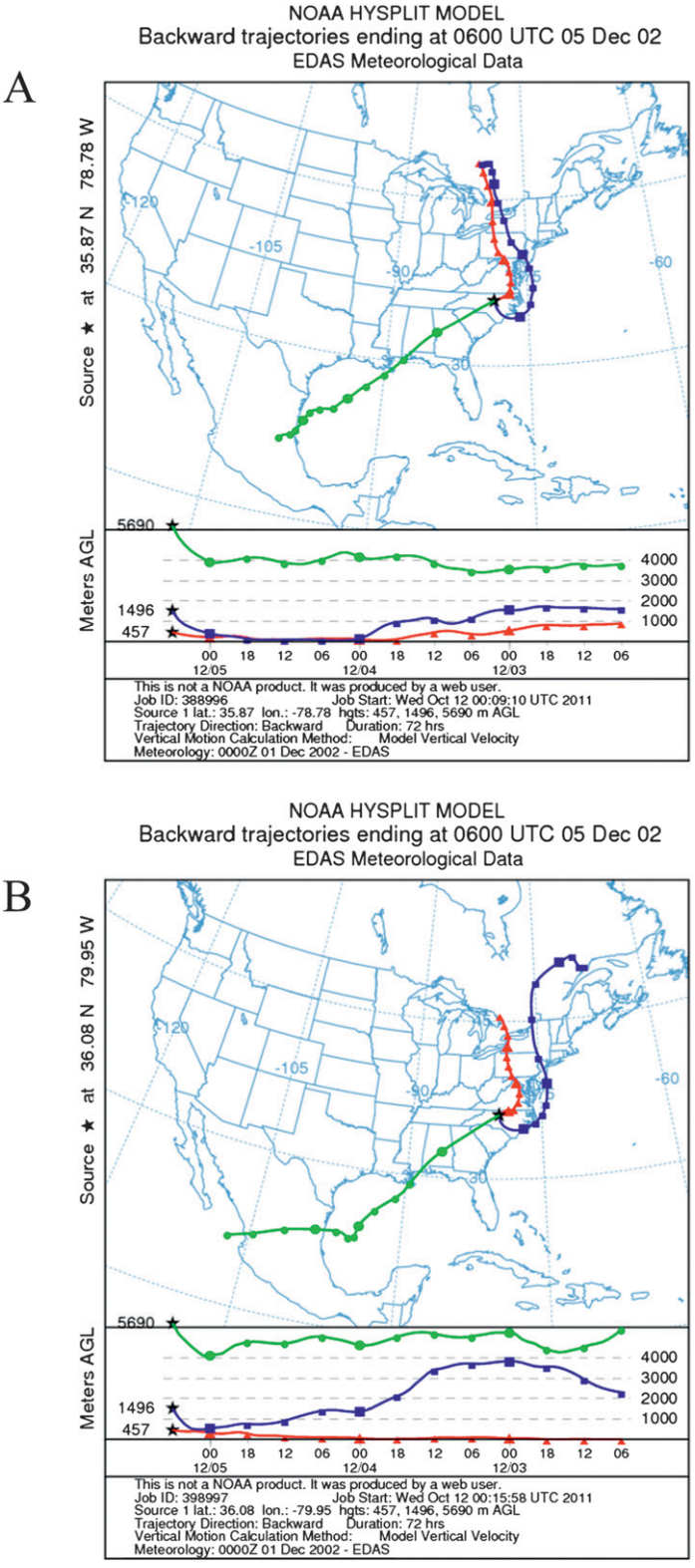

FIG. 14. As in Fig. 8, but for 0600 UTC 5 Dec 2002 at (a) RDU and (b) GSO.

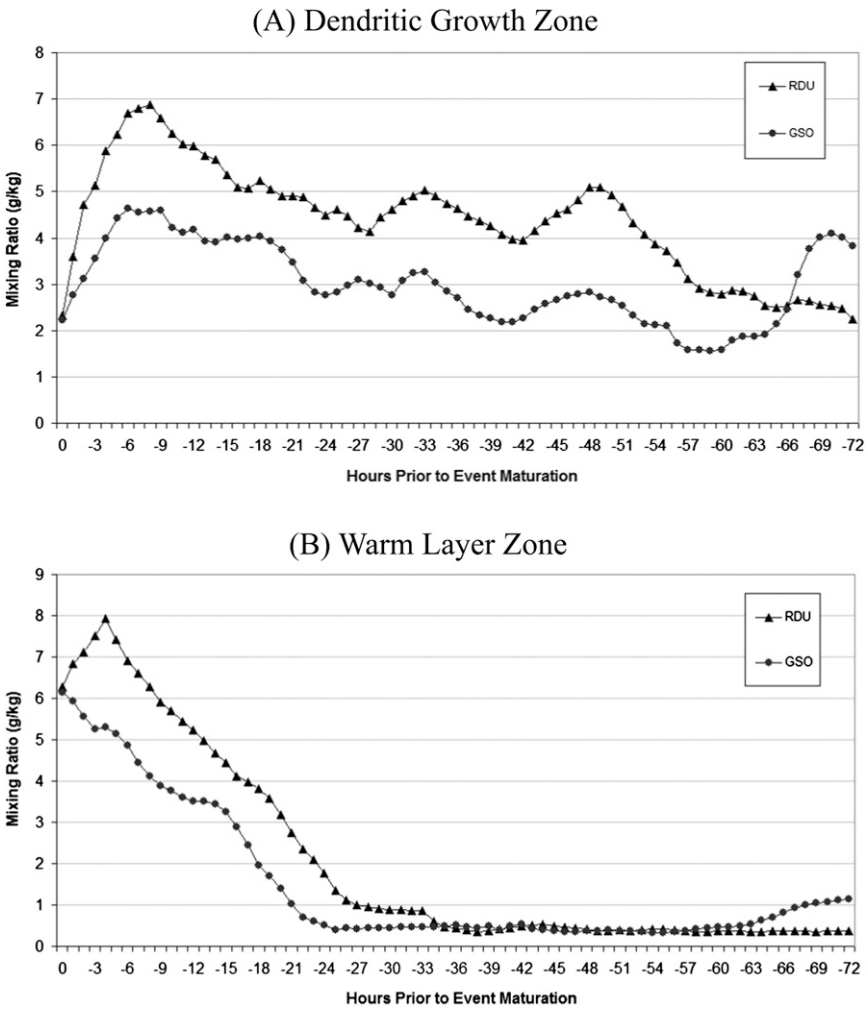

FIG. 15. As in Fig. 9, but for 0600 UTC 5 Dec 2002 terminating in the (a) dendritic growth zone and (b) WLZ at RDU and GSO.

latent heat fluxes contributed to warmer parcel temperatures and higher moisture contents compared to the closest historical circulation analogs.

The variability in the space–time character of the DGZ trajectory resulted in varying meteorological properties and, therefore, varying precipitation rates. Snowstorms with a DGZ-cyclonic trajectory originated within the MABL (<1 km) over the warm waters of the Caribbean Sea. These trajectories exhibited large overall moisture contents, strong vertical velocities, and well-defined evaporation–precipitation cycles. This implies high rates of condensation and deposition (i.e., precipitation formation and growth). Snowstorms with a DGZ-anticyclonic trajectory also exhibited strong vertical velocities and well-defined evaporation–precipitation cycles, but transported significantly less moisture into central North Carolina. As a result, the maximum precipitation rates were generally lower. In general, air parcels originating in tropical regions (below 25°N) were able to transport nearly twice as much moisture into central North Carolina compared to those originating in the Gulf of Mexico, and more than 4 times as much moisture than those traveling off of the Northeast and mid-Atlantic coasts.

Ice storms with a DGZ-Gulf trajectory originated within the MABL over the Gulf of Mexico. These trajectories exhibited large overall moisture contents, modest vertical velocities associated with isentropic lifting, and well-defined evaporation–precipitation cycles. Conversely, the DGZ-Pacific trajectory originated above the MABL (>3 km) over the eastern Pacific Ocean near the west coast of Mexico. As a result, these trajectories transported less moisture into central North Carolina. Maximum precipitation rates were, therefore, significantly lower. In general, air parcels that descended below

2 km over the Gulf of Mexico exhibited more than twice the amount of moisture observed in air parcels that remained above 2 km.

Compared to the snowstorm cases, ice storms exhibited lower maximum moisture contents and vertical velocities in the DGZ but higher overall maximum precipitation rates. This may be explained through examination of the WLZ trajectories. Ice storms exhibited a decrease in moisture content and an increase in upward vertical velocity over the final 6 h of the trajectory. This suggests that some of moisture in the WLZ was converted to rain droplets (i.e., warm cloud precipitation formation) and seeded by falling hydrometeors from the DGZ above (i.e., cold cloud precipitation formation). The combined influence of warm cloud and cold cloud precipitation formation processes could explain the higher maximum precipitation rates in these cases (Stewart 1992).

Atmospheric trajectories have been shown to be good indicators of synoptic-scale circulation regimes (Roberge et al. 2009). Therefore, it is likely that various features of the large-scale circulation, including subtle ones, may be useful in predicting trajectory motions. These include the positioning and strength of troughs and ridges as well as the tracking and intensity of surface cyclones and anticyclones. We intend to explore the relationships between the trajectory motions and various synoptic-scale circulation features in a follow-up study. On the other hand, there may be greater uncertainty in the predictability of trajectories at the mesoscale due to the increased sensitivity of the trajectory input data to boundary layer processes, zones of enhanced upward vertical motion, and small-scale fluxes of heat and moisture. Future work should include mesoscale model simulations of trajectory motions and meteorological variables using various sensible and latent heat flux parameters. A mesoscale model could also help diagnose the role of instability and convection on the trajectory motions and resulting precipitation characteristics.

While the results of this study may be applicable to forecasters in the southeast United States, the trajectory framework established here may prove useful in other regions as well and for a variety of precipitation forecast scenarios. Currently, the Air Resource Laboratory produces 36-h forecast trajectories at 6-h intervals using the North American Mesoscale Model. Forecasters could calculate specific meteorological parameters, including adiabatic and diabatic temperature changes, along each forecast trajectory using a gridded forecast product of their choice to determine the temperature near the surface and of the WLZ, as well as calculate rates of condensation and deposition in the DGZ. While we found the 975- and 850-hPa levels to be appropriate in diagnosing the air associated with the near-surface environment and WLZ in the Raleigh, North Carolina, CWA, respectively, the trajectory approach allows the forecaster to select whatever altitudes they feel are most appropriate for their region and forecast scenario. Additionally, as an event unfolds, forecasters can run multiple trajectories (i.e., ensembles) with up-to-date forecast model output to determine the likely precipitation scenarios at different locations and at different stages of the event.

Acknowledgments. We thank John Bane, Scott Curtis, Peter Robinson, Marshall Shepherd, and Tom Whitmore for their valuable feedback on the development of this study. Baker Perry, Brandon Locklear, John Cortinas, and Gary Lackmann also provided useful insight on winter precipitation processes and forecasting challenges. We greatly appreciate the efforts of three anonymous reviewers, whose comments and suggestions significantly improved the manuscript.

REFERENCES

Auer, A. H., and J. M. White, 1982: The combined role of kinematics, thermodynamics, and cloud physics associated with heavy snowfall episodes. *J. Meteor. Soc. Japan,* **60,** 500–507.

Bane, J. M., Jr., and K. E. Osgood, 1989: Wintertime air–sea interaction processes across the Gulf Stream. *J. Geophys. Res.,* **94** (C8), 10 755–10 772.

Bell, G. D., and L. F. Bosart, 1988: Appalachian cold-air damming. *Mon. Wea. Rev.,* **116,** 137–161.

Black, T. L., 1994: The new NMC mesoscale Eta Model: Description and forecast examples. *Wea. Forecasting,* **9,** 265–278.

Brennan, M. J., and G. M. Lackmann, 2005: The influence of incipient latent heat release on the precipitation distribution of the 24–25 January 2000 U.S. East Coast cyclone. *Mon. Wea. Rev.,* **133,** 1913–1937.

Buzzia, R., and P. Chessa, 2002: Prediction of the U.S. storm of 24–25 January 2000 with the ECMWF Ensemble Prediction System. *Mon. Wea. Rev.,* **130,** 1531–1551.

Draxler, R. R., 2003: Evaluation of an ensemble dispersion calculation. *J. Appl. Meteor.,* **42,** 308–317.

——, and G. D. Rolph, cited 2011: HYSPLIT-Hybrid Single-Particle Lagrangian Integrated Trajectory Model. [Available online at http://ready.arl.noaa.gov/HYSPLIT.php.]

Field, G. A., and J. D. Stewart, 1994: Evaluation of an unusual winter weather non-occurrence in North Carolina on 24 January 1991. *Natl. Wea. Dig.,* **19** (1), 2–13.

Fritsch, J. M., and Coauthors, 1998: Quantitative precipitation forecasts: Report of the Eighth Prospectus Development Team, U.S. Weather Research Program. *Bull. Amer. Meteor. Soc.,* **79,** 285–299.

Fuhrmann, C. M., 2011: A trajectory approach to analyzing the ingredients associated with heavy winter storms in central North Carolina. Ph.D. dissertation, University of North Carolina at Chapel Hill, 239 pp.

——, R. P. Connolly, and C. E. Konrad, 2009: Winter storms: An overlooked source of death, destruction, and inconvenience in the Carolina Piedmont region. *Proc. 66th Eastern Snow Conf.,* Niagra-on-the-Lake, ON, Canada, ESC, 45–58.

Gyakum, J. R., and P. J. Roebber, 2001: The 1998 ice storm—Analysis of a planetary-scale event. *Mon. Wea. Rev.,* **129,** 2983–2997.

Hondula, D. M., and Coauthors, 2009: A back-trajectory and air mass climatology for the northern Shenandoah Valley, USA. *Int. J. Climatol.,* **30,** 569–581.

James, P., A. Stohl, N. Spichtinger, S. Eckhardt, and C. Foster, 2004: Climatological aspects of the extreme European rainfall of August 2002 and a trajectory method for estimating the associated evaporative source regions. *Nat. Hazards Earth Syst. Sci.,* **4,** 733–746.

Kain, J. S., S. M. Goss, and M. E. Baldwin, 2000: The melting effect as a factor in precipitation-type forecasting. *Wea. Forecasting,* **15,** 700–714.

Keeter, K. K., S. Businger, and L. G. Lee, 1993: Patterns of winter precipitation types across North Carolina. Preprints, *13th Conf. on Weather Analysis and Forecasting,* Vienna, VA, Amer. Meteor. Soc., 528-532.

——, ——, ——, and J. S. Waldstreicher, 1995: Winter weather forecasting throughout the eastern United States. Part III: The effects of topography and the variability of winter weather in the Carolinas and Virginia. *Wea. Forecasting,* **10,** 42–60.

Kocin, P. J., and L. W. Uccellini, 2004: *Northeast Snowstorms.* Vol. 1, *Meteor. Monogr.,* No. 54, Amer. Meteor. Soc., 296 pp.

Lackmann, G. M., 2006: Improving cold-season quantitative precipitation forecasting in the southeastern United States. Final report on the proposal to NOAA in support of the Collaborative Science, Technology, and Applied Research Program (CSTAR), 18 pp. [Available online at http://www4.ncsu.edu/~nwsfo/storage/resupdates/Revised_NCSU_CSTAR_II_Final_Report.pdf.]

——, K. K. Keeter, L. G. Lee, and M. B. Ek, 2002: Model representation of freezing and melting precipitation: Implications for winter weather forecasting. *Wea. Forecasting,* **17,** 1016–1033.

Market, P. S., R. W. Przybylinski, and S. M. Rochette, 2006: The role of sublimational cooling in a late-season Midwestern snow event. *Wea. Forecasting,* **21,** 364–382.

Moore, J. T., S. Ng, and C. E. Graves, 2005: The role of conveyor belts in organizing processes associated with heavy banded snowfall. Preprints, *21st Conf. on Weather Analysis and Forecasting,* Washington, DC, Amer. Meteor. Soc., 10A.1. [Available online at https://ams.confex.com/ams/WAFNWP34BC/techprogram/paper_94644.htm.]

Perry, L. B., 2006: Synoptic climatology of northwest flow snowfall in the southern Appalachians. Ph.D. dissertation, University of North Carolina at Chapel Hill, 192 pp.

Richwien, B. A., 1980: The damming effect of the southern Appalachians. *Natl. Wea. Dig.,* **5** (1), 2–12.

Robbins, C. C., and J. V. Cortinas, 2002: Local and synoptic environments associated with freezing rain in the contiguous United States. *Wea. Forecasting,* **17,** 47–65.

Roberge, A., J. Gyakum, and E. Atallah, 2009: Analysis of poleward water vapor transport into high latitudes of western North America. *Wea. Forecasting,* **24,** 1732–1747.

Rogers, E., and Coauthors, 2009: The NCEP North American mesoscale modeling system: Recent changes and future plans. Preprints, *23rd Conf. on Weather Analysis and Forecasting,* Omaha, NE, Amer. Meteor. Soc., 2A.4. [Available online at https://ams.confex.com/ams/pdfpapers/154114.pdf.]

Ryerson, C. C., and A. C. Ramsay, 2007: Quantitative ice accretion information from the Automated Surface Observing System. *J. Appl. Meteor. Climatol.,* **46,** 1423–1437.

Schultz, D. M., 2001: Reexamining the cold conveyor belt. *Mon. Wea. Rev.,* **129,** 2205–2225.

Stewart, R. E., 1992: Precipitation types in the transition region of winter storms. *Bull. Amer. Meteor. Soc.,* **73,** 287–296.

Stohl, A., 1998: Computation, accuracy and applications of trajectories—A review and bibliography. *Atmos. Environ.,* **32,** 947–966.

Waldstreicher, J. S., 2005: Assessing the impact of collaborative research projects on NWS warning performance. *Bull. Amer. Meteor. Soc.,* **86,** 193–203.